Catalysis Science & Technology

Determining Intrinsic Stark Tuning Rates of Adsorbed CO on Copper Surfaces

Journal:	*Catalysis Science & Technology*
Manuscript ID	CY-ART-06-2021-001090.R1
Article Type:	Paper
Date Submitted by the Author:	12-Aug-2021
Complete List of Authors:	Chang, Xiaoxia; University of Delaware Xiong, Haocheng; Tsinghua University, Department of Chemical Engineering Xu, Yifei; Peking University, College of Chemistry and Molecular Engineering Zhao, Yaran; University of Delaware, Chemical Engineering Lu, Qi; Tsinghua University, Department of Chemical Engineering Xu, Bingjun; Peking University, College of Chemistry and Molecular Engineering

Determining Intrinsic Stark Tuning Rates of Adsorbed CO on Copper Surfaces

Xiaoxia Chang[1,2,3], Haocheng Xiong[1,2,4], Yifei Xu[1,2], Yaran Zhao[3], Qi Lu[4,*] and Bingjun Xu[1,2,3,*]

[1]College of Chemistry and Molecular Engineering, Peking University, Beijing, 100871, China
[2] Beijing National Laboratory for Molecular Sciences, Beijing, 100871, China
[3]Center for Catalytic Science and Technology, Department of Chemical and Biomolecular Engineering, University of Delaware, Newark, Delaware 19716, United States
[4]State Key Laboratory of Chemical Engineering, Department of Chemical Engineering, Tsinghua University, Beijing 100084, China

*Corresponding authors: luqicheme@mail.tsinghua.edu.cn, b_xu@pku.edu.cn

Abstract

The abrupt change in potential between the electrode and the electrolyte, and the resulting interfacial electric field, is the driving force in electrochemical reactions. For surface mediated electrocatalytic reactions, the interfacial electric field is believed to have a key impact on the stability and reactivity of adsorbed intermediates. However, the exact mechanisms remain a topic of discussion. In this context, reliable measurements of the interfacial electric field are a prerequisite in understanding how it influences the rate and product distribution in electrochemical reactions. The vibrational Stark effect of adsorbates, such as CO, offers an accessible means to assess the interfacial electric field strength by determining the shift of vibrational peaks of the adsorbates with potential, i.e., the Stark tuning rate. However, the vibrational Stark effect could be convoluted with the dynamical dipole coupling effect of the adsorbates on weak binding surfaces such as Cu, thus complicating the determination of the intrinsic Stark tuning rate. In this work, we report a general and effective strategy of determining the intrinsic Stark tuning rate by removing the impact of the dynamical coupling of adsorbed CO on Cu surface with surface enhanced infrared absorption spectroscopy. A similar intrinsic Stark tuning rate of ~33 cm^{-1}/V was obtained on oxide-derived Cu in different electrolyte pH of 7.2, 10.9 and 12.9, indicating the pH independence of the interfacial electric field. Investigations on different Cu electrodes show that the intrinsic Stark tuning rates on (electro)chemically deposited films are close to 33 cm^{-1}/V, while particulate Cu catalysts show a similar value of ~68 cm^{-1}/V. These observations indicate the aggregate morphology, rather than the size and shape of individual catalyst particles, has a more prominent impact on the interfacial electric field.

Introduction

Heterogeneous electrochemical processes are driven by the potential change at the electrode/electrolyte interface. Due to the buildup of the electric double layer and the effective screening of solvent molecules, e.g., water, the majority of potential changes occur between the outer Helmholtz layer and the electrode surface (within a few Angstroms), resulting in immense interfacial electric fields.[1] The interfacial electric field is a major driving force in electrochemical reactions, and thus its reliable measurement and modeling are of considerable theoretical and practical importance.[2,3] For example, the effect of cations in the electrochemical CO and CO_2 reduction reactions ($CO_{(2)}RR$) on the reaction rate and product selectivity has been related to the strength of the interfacial electric field,[4,5] though it is unlikely the sole or dominant factor.[6,7] Aside from impacting the stability of adsorbed intermediates, the interfacial electric field also impacts the energetics of their vibrational modes, known as the vibrational Stark effect.[8,9] This provides a convenient way to gauge the dependence of the interfacial electric field strength on the potential via in-situ electrochemical infrared or Raman spectroscopies by monitoring the rate at which peak frequency varies with potential, i.e., the Stark tuning rate. Adsorbed CO is a suitable probe molecule, as well as an intermediate in the $CO_{(2)}RR$, owing to its large dipole moment and sensitive interaction with the substrate.[10-12] The frequency of the stretching mode of adsorbed CO varies with the electrode potential, which is also impacted by the shift of the Fermi level in the metal and in turn the back donation from the metal electrode to the $2\pi^*$ antibonding orbital of CO.[13-16] This electronic effect cannot be differentiated from the electric effect because they always coexist under any given electrochemical conditions. For example, Su *et al.* employed in-situ Raman spectroscopy to show that the Stark tuning rates of CO on Pt(111) and Pt(100) are significantly higher than that on Pt(110) (30 cm^{-1}/V vs. 20 cm^{-1}/V), providing mechanistic understanding into

the higher CO electrooxidation activity on the former two surfaces.[17] In addition to Raman spectroscopy, surface enhanced infrared absorption spectroscopy (SEIRAS) provides another highly interfacial sensitive tool to identify the adsorbate species on the molecule level.[18] We recently demonstrated with in-situ SEIRAS that the Stark tuning rate of CO adsorbed on Cu increased from Li^+ to K^+ and then leveled off for larger cations of Rb^+ and Cs^+. Given the monotonically increasing CORR activity with the cation size from Li^+ to Cs^+, we proposed that a nonelectric field strength component is also at play in the cation effect on CORR activity,[6] which is line with a recent report.[7]

The growing popularity of Stark tuning measurements on non-precious metal surfaces, e.g., Cu in the $CO_{(2)}RR$,[19] calls for more robust experimental procedures to extract reliable Stark tuning rate values. It is important to note that it is often difficult to isolate a variable in electrochemical systems because species interact extensively in the electric double layer. For example, varying potential could easily change the surface coverage of a given adsorbate. Surface coverage is known to impact the wavenumber of vibrational bands via the dynamical dipole coupling,[20,21] and thus reliable Stark tuning rates can only be obtained at a constant coverage of the probe molecule. This requirement does not pose much challenge for CO adsorbed on precious metals due to its strong binding, i.e., a constant saturation coverage could be maintained in a sufficiently wide potential window to determine Stark tuning rates.[16] The situation is considerably different for weak binding surfaces, on which the adsorbate coverage could vary substantially with potential. In such cases, peak shifts with potential, i.e., the apparent Stark tuning rate, could be caused by both the vibrational Stark effect and the coverage effect. Therefore, peak shift attributable to potential changes at a constant coverage, i.e., the intrinsic Stark tuning rate, needs to be determined by removing the contribution of the coverage effect from the apparent Stark tuning rate. Only the

intrinsic Stark tuning rate, rather than the apparent Stark tuning rate, is a reliable measure of the rate at which the interfacial electric field strength varies with potential, which could be related to materials' electrocatalytic performances.

In this work, we report a general and reliable strategy to remove the coverage effect from measured apparent Stark tuning rates of adsorbed CO bands on Cu electrodes via in-situ SEIRAS. The correlation between the integrated CO peak area and position was determined by varying the CO partial pressure, and in turn the surface coverage, at a constant potential. This quantitative correlation was then used as a calibration curve to correct the peak wavenumbers determined at different potentials. Intrinsic Stark tuning rates can then be obtained by the linear fitting of the corrected band wavenumber vs. the applied potential. Using this strategy, a similar intrinsic Stark tuning rate of ~33 cm^{-1}/V was obtained for CO adsorption on oxide-derived Cu (OD-Cu) in different electrolyte pH of 7.2, 10.9 and 12.9, indicating the pH independence of the interfacial electric field. Furthermore, we investigated the intrinsic Stark tuning rates on four different Cu electrodes under the same conditions, including chemically deposited Cu film (Chem-Cu), electrochemically deposited OD-Cu film, dropcast dendritic Cu (Den-Cu) and Cu microparticles (Cu MPs). (Electro)chemically deposited films show a similar rate of ~33 cm^{-1}/V, while electrodes prepared by dropcasting catalyst inks exhibit a similar value of ~68 cm^{-1}/V. These observations indicate that the electrode aggregate morphology, rather than the size and shape of individual particles, has a substantial impact on the interfacial electric field.

Results and Discussion

Correction of CO Band Wavenumber on OD-Cu in Different Electrolyte pH

OD-Cu films were prepared via the electrochemical reduction of a Cu_2O film that was pre-deposited on Au film for SEIRAS (detailed synthesis procedure reported elsewhere[22,23] and

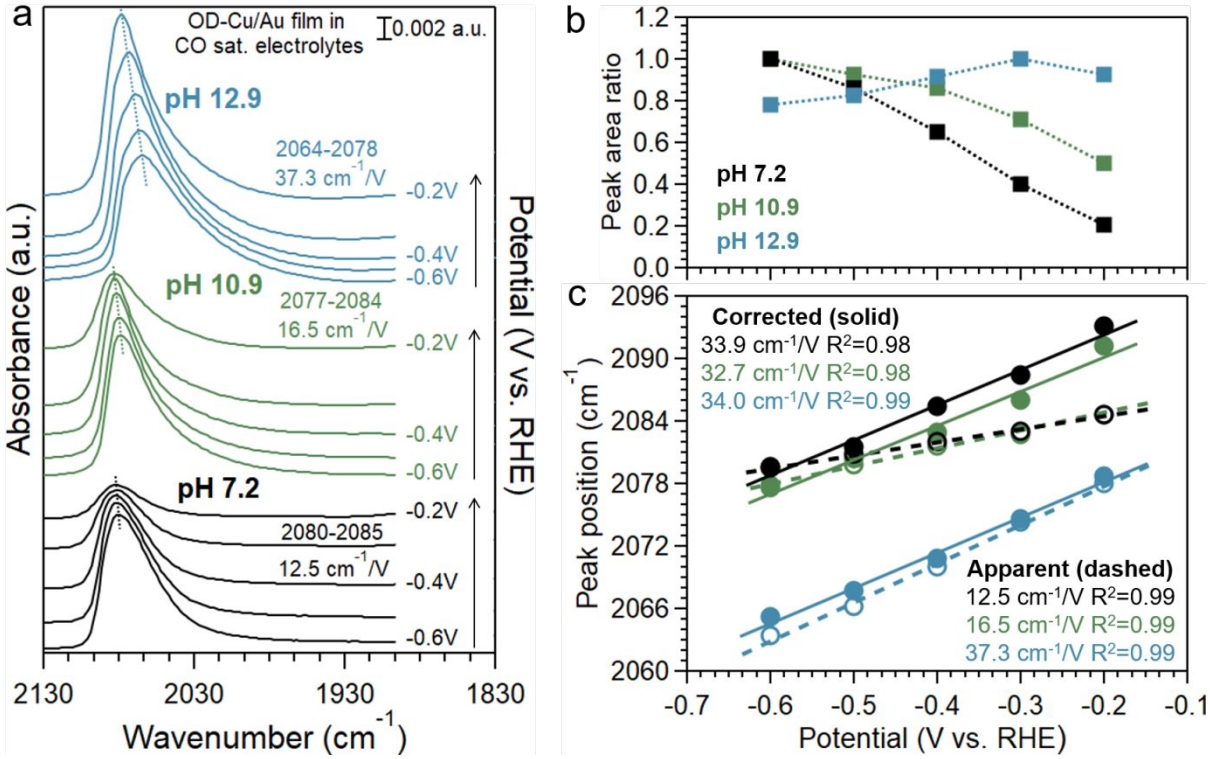

Figure 1. (a) In-situ SEIRA spectra of CO adsorption on OD-Cu in 0.03 M NaH_2PO_4 + 0.035 Na_2HPO_4 (pH = 7.2, black traces), 0.05 Na_2CO_3 (pH = 10.9, green traces) and 0.1 NaOH (pH = 12.9, blue traces) at potentials indicated in the figure. The spectra were collected at constant potentials with 0.1 V intervals in the anodic direction from the -0.6 to -0.2 V_{RHE}. (b) The normalized peak area of CO adsorption bands in different electrolyte pH as a function of potential. (c) The apparent (hollow circles and dashed lines) and corrected (solid circles and lines) potential dependence of CO band frequency. Stark tuning rates are determined through the linear fits of the point data.

included in the Supporting Information). The Stark tuning rate of CO band on OD-Cu was determined in three distinct electrolyte pH with a constant Na^+ concentration of 0.1 M: 0.03 M NaH_2PO_4 + 0.035 M Na_2HPO_4 (pH = 7.2), 0.05 M Na_2CO_3 (pH = 10.9) and 0.1 M NaOH (pH = 12.9). All the spectra were collected in a custom-designed, stirred spectroelectrochemical cell to enhance the mass-transfer in the electrolyte (Figure S1). The spectra in CO saturated electrolytes with different pH are shown in Figure 1a, in which the potential scans anodically from -0.6 to -0.2 V vs. the reversible hydrogen electrode (V_{RHE}). The band located in the region of 2000-2100 cm^{-1} is attributed to the linearly bound CO on the atop sites of Cu surface (CO_{atop}), whose intensity varies with the applied potential.[24,25] In the electrolytes with pH 7.2 and 10.9, the intensity of CO

band reaches the maximum at -0.6 V_{RHE} in the potential range investigated and decreases with the anodic potential shift (black and green traces in Figure 1b, respectively). Compared to the case in an electrolyte pH of 10.9, CO band in pH 7.2 changes more rapidly in intensity with only 20% left at -0.2 V_{RHE}. Further increasing the electrolyte pH to 12.9 significantly broadens the CO bands (blue traces in Figure 1a), which can be an indication of the Cu surface becoming less homogeneous in the strongly alkaline electrolyte.[23,26] In addition, CO band in pH 12.9 shows an increased intensity and a visible redshift of peak position (blue traces in Figure 1a and c) compared to that in less alkaline electrolytes, which are expected because the absolute potential is lower in the more alkaline electrolyte at a given RHE potential. The intensity reaches the maximum at -0.3 V_{RHE} and shows negligible change with the potential (blue trace in Figure 1b). In all the electrolytes investigated, the peak frequency of CO band blueshifts as the potential increasing from -0.6 to -0.2 V_{RHE}, resulting in the apparent Stark tuning rates of 12.5, 16.5 and 37.3 cm^{-1}/V in electrolyte pH of 7.2, 10.9 and 12.9, respectively (dashed lines in Figure 1c). These observations raise the question whether the interfacial electric field strength is dependent on the electrolyte pH value. It is important to note that the shift of the CO band position with the applied potential can be caused by both the coverage effect, i.e., the dynamical dipole coupling,[20,21] and Stark tuning effect,[27,28] of which only the latter is induced by the interfacial electric field. Given the substantial change in the peak area with the potential, the dynamical dipole coupling among adsorbed CO at different coverages is expected to have a strong impact on the shift of peak position. Thus, in order to obtain the intrinsic Stark tuning rates as a reliable experimental measure of the interfacial electric field strength, the coverage effect needs to be removed from the apparent Stark tuning rates. It is worth noting that the asymmetrical lineshapes of CO bands in Figure 1a indicate the heterogeneities of Cu surface sites, the Stark tuning rates determined in this work represent the average values of all

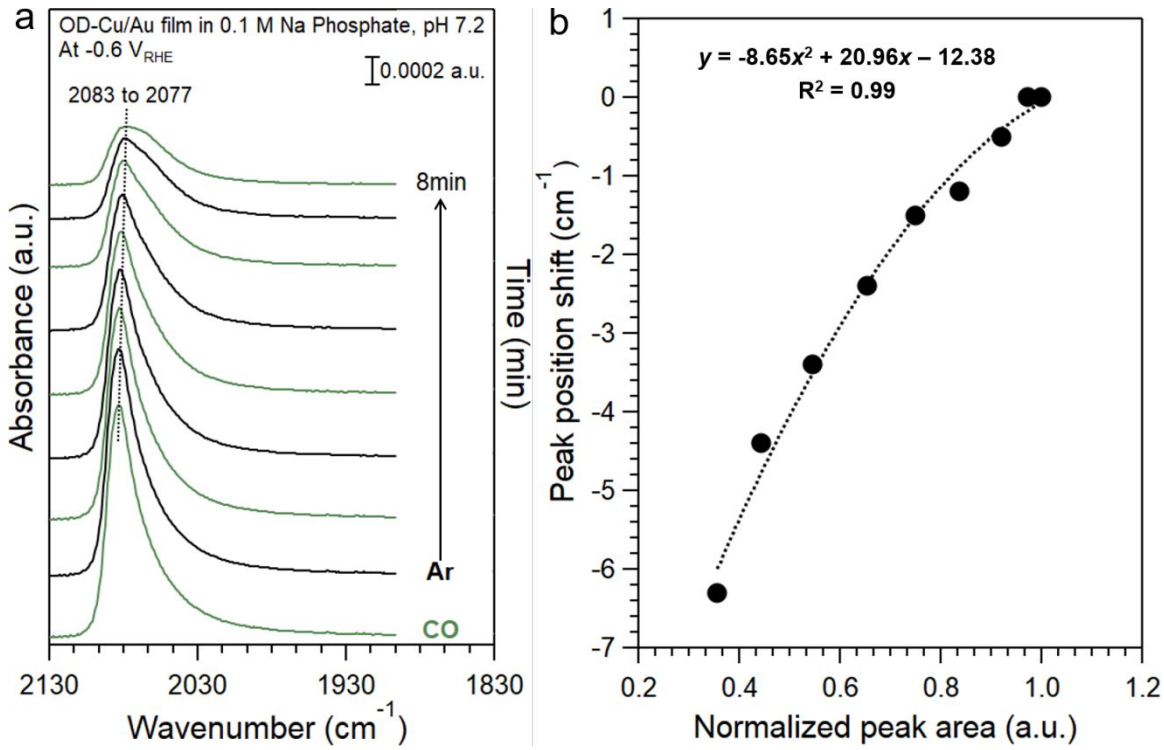

Figure 2. (a) In-situ SEIRAS study on the peak area dependence of CO band frequency via switching the bubbling gas to Ar on OD-Cu at -0.6 V_{RHE} in 0.03 M NaH_2PO_4 + 0.035 M Na_2HPO_4 (pH = 7.2). (b) The peak position shift from that under CO as a function of the peak area. The second-order polynomial fitting of the point data is shown as dashed line. The spectral resolution is set at 2 cm^{-1} for an accurate calibration.

available surface sites.

The coverage correction of the measured apparent Stark tuning rates could be achieved by determining a relative peak area vs. peak position curve at a given potential (Figure 2). For example, CO adsorption spectra were initially collected in CO saturated 0.1 M sodium phosphate buffer under -0.6 V_{RHE}, at which the intensity of CO band is maximum in this electrolyte (Figure 1b). After reaching equilibrium, Ar was introduced into the electrolyte to substitute CO and the SEIRA spectra were collected continuously with the time. The CO band gradually decreases due to the consumption of CO in the CORR or desorption, accompanied by a redshift of the peak position from 2083 to 2077 cm^{-1} induced by the decoupling of adsorbed CO in the adlayer (Figure 2a). It is worth noting that the small frequency shift of only ~6 cm^{-1} with the peak area reducing to ~35%

of its maximum indicates a weak dynamical dipole coupling and low absolute surface coverage of CO.[20,29,30] The minor difference in the peak frequency at -0.6 V_{RHE} between the spectra in Figure 1a and Figure 2a is likely attributed to the film-to-film variations, while the apparent Stark tuning rates are highly consistent among different films. The calibration curve can be obtained by fitting the peak area dependence of the peak position shift from those under CO gas (the bottom trace in Figure 2a), through which a second-order polynomial $f(x)$ with a R-squared value of 0.99 is determined (Figure 2b). It is worthy to note that the spectra where CO_{atop} dominates were selected to determine the calibration curve, thus excluding any impact from the change of lineshape caused by CO adsorbed on different sites (Figure 2a). We also show that this curve is largely independent of the potential chosen by conducting the same experiment at -0.3 V_{RHE} (Figure S2). The wavenumbers of CO bands collected at different potentials are corrected with $f(x)$ according to the following equation:

$$\upsilon_{cor.} = \upsilon_{app.} - f\left(S_E \middle/ S_{E_{max}}\right) \quad (1)$$

where $\upsilon_{cor.}$ and $\upsilon_{app.}$ are the corrected and as-measured peak wavenumbers, respectively. S_E is the integrated peak area of CO band at a given electrode potential E, and $S_{E_{max}}$ is the maximum peak area of CO band in the potential range investigated. Thus, the term $\frac{S_E}{S_{E_{max}}}$ stands for the normalized peak area as the X-axis of Figure 2b. The intrinsic Stark tuning rate can be determined with the corrected wavenumbers ($\upsilon_{cor.}$).

The Stark tuning rate in pH 7.2 increases from 12.5 to 33.9 cm^{-1}/V after the correction of peak frequencies due to the CO coverage effect (black solid line in Figure 1c). Applying the same correction strategy, the Stark tuning rates in pH 10.9 and 12.9 are corrected to be 32.7 and 34.0 cm^{-1}/V, respectively (green and blue solid lines in Figure 1c), with the calibration curves shown in

Figures S3 and S4. These values are referred to as the intrinsic Stark tuning rates in this work. The minor change of Stark tuning rate in pH 12.9 upon the correction (from 37.3 cm^{-1}/V to 34.0 cm^{-1}/V) is due to the similar intensity of CO band and thus an insignificant coverage effect in the potential range of -0.6 to -0.2 V_{RHE} (blue trace in Figure 1b). The similar intrinsic Stark tuning rates (~33.0 cm^{-1}/V) obtained in the pH range of 7.2-12.9 indicate that surface adsorbed CO experiences a similar change within the interfacial electric field in this potential range. In addition, the intrinsic Stark tuning rate was determined to be the same within the experimental errors at a CO partial pressure of of 0.5 atm, showing its independence regarding the p_{CO} and in turn the absolute coverage of CO in electrochemical systems (Figure S5). Interestingly, OD-Cu surface appears very sensitive to the chemicals used in the preparation procedure. For example, replacing the DL-lactic acid with L-lactic acid in the electrodeposition bath for Cu_2O film led to a significantly higher apparent Stark tuning rate of 28.1 cm^{-1}/V in 0.05 M Na_2CO_3 (vs. 16.5 cm^{-1}/V with the DL-lactic acid, Figure 1). The intrinsic Stark tuning rate is determined to be 34.1 cm^{-1}/V after the correction (Figure S6), close to the observed value of ~33 cm^{-1}/V on the OD-Cu prepared with DL-lactic acid (Figure 1c).

Several points deserve further discussion regarding the observation of the pH independence of interfacial electric field strength. All three electrolytes used in the experiments described above contain 0.1 M Na^+, thus no different impact of cation on the interfacial electric field is expected. Moreover, the negative potentials (-0.6 to -0.2 V_{RHE}) at which Stark tuning rate is determined makes the specific adsorption of anions unlikely because they are electrostatically repelled from the electrode surface.[31] We note that the specific adsorption of phosphate at negative potentials was observed in a high concentration phosphate solution of 1.0 M using surface enhanced Raman spectroscopy (SERS) in our recent work.[26] The diluted solution (0.1 M) employed in this work

makes the specific adsorption of anions less likely to have a strong impact on the interfacial electric field at reducing potentials. Further, we showed that the surface speciation of Cu has a strong pH dependence, showing an increasing propensity to form surface oxygen-containing species at $CO_{(2)}RR$ conditions with the increase of electrolyte pH from 8.9 to 12.6.[23,32] Given the constant interfacial electric field with the change of electrolyte pH between 7.2 and 12.9 in this work, the surface oxygen-containing species is unlikely to play any major role in affecting the interfacial electric field.

Dependence of Intrinsic Stark Tuning Rates on Sample Morphology

In addition to OD-Cu, we also determined the intrinsic Stark tuning rates of CO band on other three kinds of Cu surfaces: Chem-Cu, Cu MPs and Den-Cu in 0.1 M NaOH (pH = 12.9). Chem-Cu electrode was obtained through the chemical deposition of Cu film onto a Si prism surface, while Cu MPs and Den-Cu electrodes were prepared by dropcasting the catalyst inks onto an SEIRA active Au film (synthesis procedure included in the Supporting Information). Among these electrodes, only Cu MPs show a strong potential dependence of CO band intensity with the maximum at -0.2 V_{RHE}, which results in a substantial difference in the apparent and intrinsic Stark tuning rates, being 74.9 and 66.1 cm^{-1}/V, respectively (Figure S7). Changes in the integrated area of CO bands on Den-Cu and Chem-Cu with potential are minor (less than 20%) in the investigated potential range of -0.6 to -0.2 V_{RHE} (Figure S8a and b, Figure S9a and b), indicating a weak coverage effect and minor corrections in the apparent Stark tuning effect (Figures S8c). Intrinsic Stark tuning rates of CO bands on different Cu surfaces appear to depend on the sample preparation methods. Samples that are chemically or electrochemically deposited on the surface of the ATR crystals, including Chem-Cu and OD-Cu films, exhibit intrinsic Stark tuning rates of ~33 cm^{-1}/V,

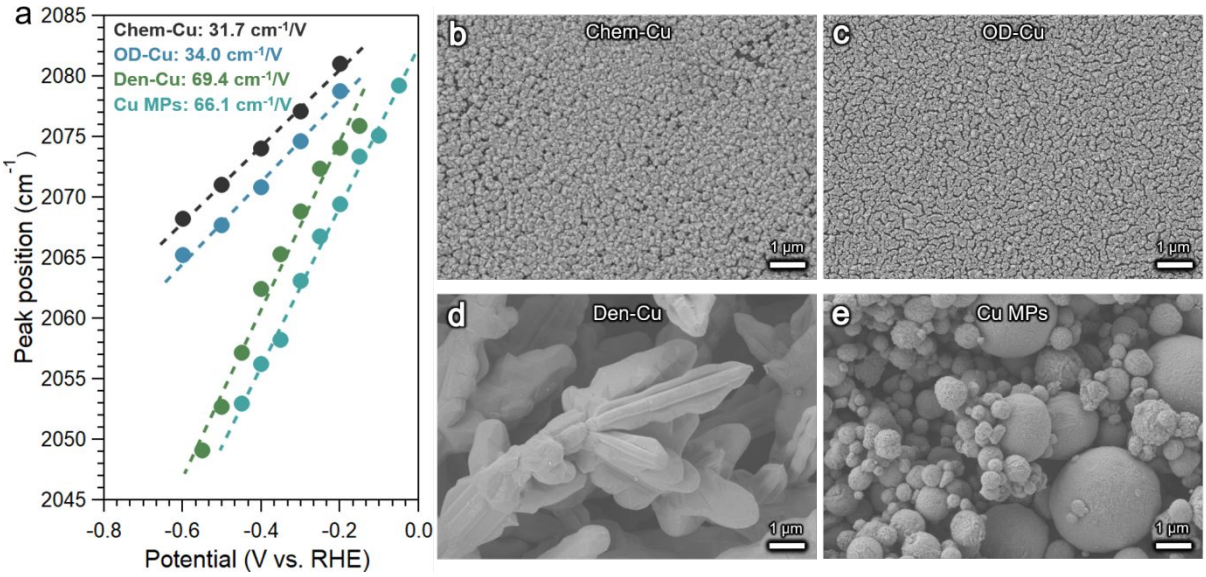

Figure 3. (a) Intrinsic Stark tuning rates of CO bands on Chem-Cu (black), OD-Cu (blue), Den-Cu (green) and Cu MPs (cyan) in 0.1 M NaOH (pH = 12.9). (b-e) SEM images of Chem-Cu, OD-Cu, Den-Cu and Cu MPs, respectively.

while particulate samples dropcast on Au films, including Den-Cu and Cu MPs, tend to have intrinsic Stark tuning rate values of ~68 cm^{-1}/V (Figure 3a). The drastic difference in the intrinsic Stark tuning rates, and in turn interfacial electric fields, among Cu surfaces is an indication that the morphology of Cu samples plays an important role. SEM images show that Cu samples prepared by chemical or electrochemical deposition (Chem-Cu and OD-Cu) exhibit relatively uniform particle size (< 200 nm) distribution and particles are closely packed together (Figure 3b and c). Meanwhile, Den-Cu and Cu MPs electrodes, prepared by dropcasting catalyst inks, show broader particle size distribution from nanometer to micrometer sized particles, and different morphologies (dendritic and spherical, Figure 3d and e). Generally, materials with high-curvature structure are known to concentrate electric fields, because the electron concentrates at the tip and its intensity increases as the electrodes sharpen. This effect originates from the migration of free electrons to the regions of the sharpest curvature on a charged metallic electrode, a consequence of electrostatic repulsion.[33] The more irregular shaped Den-Cu and Cu MPs (Figure 3d and e)

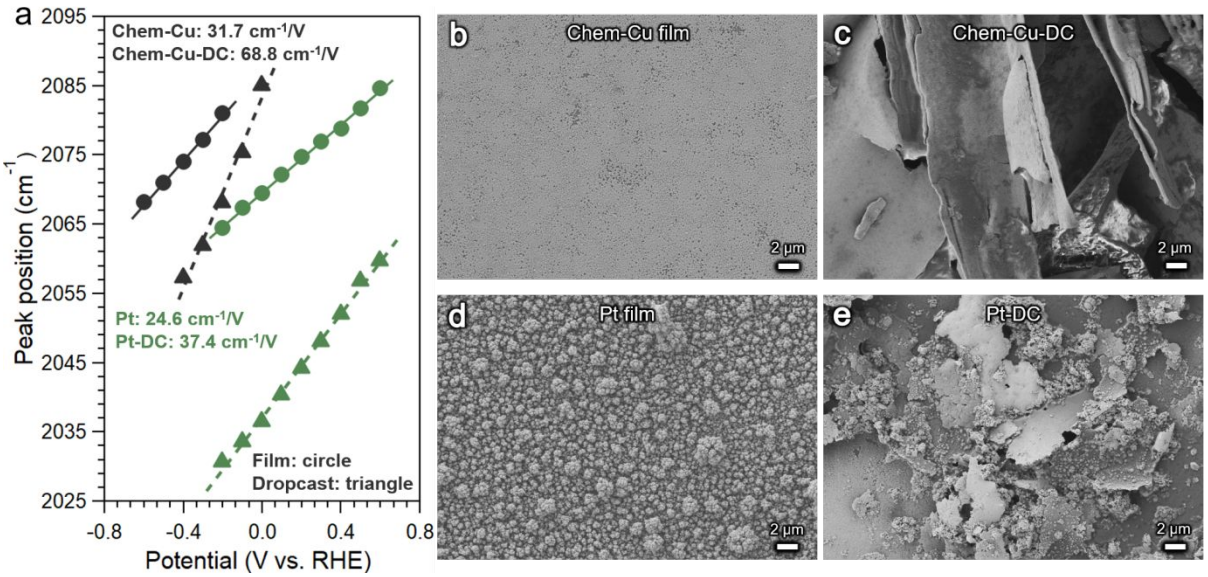

Figure 4. (a) Intrinsic Stark tuning rates of CO bands on Chem-Cu film (black circle) and Chem-Cu-DC (black triangle) in 0.1 M NaOH (pH = 12.9), as well as Pt film (green circle) and Pt-DC (green triangle) in 0.1 M $HClO_4$ (pH = 1.2). (b-e) SEM images of Chem-Cu film, Chem-Cu-DC, Pt film and Pt-DC, respectively. The DC-electrodes (c and e) were prepared by scraping the corresponding films (b and c) off Si substrate and dropcasting onto the SEIRA active Au films.

likely possess more features with local high curvature than Chem-Cu and OD-Cu (Figure 3b and c).

To further support the hypothesis that the electrode morphology, rather than the size and shape of individual particles, has a major impact on intrinsic Stark tuning rates, we conducted a series of control experiments in which these two factors were decoupled. We first prepared Chem-Cu and Pt films via chemical deposition, and then scraped them off the Si substrate. These powders were made into catalyst inks, and then dropcast onto Au films (synthesis procedure included in the Supporting Information). Through this procedure, dropcast Chem-Cu and Pt samples contain the same particle-level features as chemically deposited samples but with different morphologies and heterogeneities of aggregates (Figure 4b-e). They are referred to as Chem-Cu-DC and Pt-DC, respectively, below for clarity. Thus, any difference in the intrinsic Stark tuning rates on samples prepared by different procedures could be attributed to the difference in the aggregate morphology.

CO adsorption spectra on Chem-Cu-DC were collected in CO saturated 0.1 M NaOH at the same conditions as on the Chem-Cu sample (Figures 3a and S10). Compared to Chem-Cu (Figure S9), CO band on Chem-Cu-DC is significantly broader and redshifted (Figure S10), indicating less homogeneous adsorption sites and dynamical dipole coupling. This is consistent with the observed heterogeneous aggregate morphology (Figure 4c). The intrinsic Stark tuning rate on Chem-Cu-DC is determined to be 68.8 cm^{-1}/V (black triangle and dashed line in Figure 4a), which is more than twice as much as that on the Chem-Cu film (31.7 cm^{-1}/V) and similar to those on Den-Cu and Cu MPs (Figure 3a). This strongly suggests that the morphology of the aggregated particles is a key factor resulting in their different intrinsic Stark tuning rates. In addition to Cu surfaces, we also conducted CO adsorption on Pt film and Pt-DC in 0.1 M $HClO_4$ (Figures S11 and S12), which is a well-studied system in the literature.[28,34,35] CO band intensity on Pt barely changes within the investigated potential range of -0.2 to 0.6 V_{RHE} (Figures S11b and S12b), making the coverage correction unnecessary in this system. Pt film shows an intrinsic Stark tuning rate of 24.6 cm^{-1}/V (green circle and solid line in Figure 4a), which is consistent with the previous reports under similar conditions.[28,34] As in the case on Cu surface, CO band is significantly broadened and redshifted on Pt-DC at the same conditions (Figure S12a). The intrinsic Stark tuning rate of the CO band increases from 24.6 cm^{-1}/V on the Pt film to 37.4 cm^{-1}/V on Pt-DC (green triangle and dashed line in Figure 4a), confirming the impact of the aggregate morphology on the vibrational Stark effect (Figure 4d and e). These results demonstrate that the dependence of the interfacial electric field strength on the electrode potential is sensitive towards the morphology of the catalyst particles, which could in part account for the reported reactivity difference between foil and particulate Cu catalysts in the electrochemical reduction of CO and CO_2.[32,36,37] We note that CO Stark tuning rates on Pt(111) and Pt(110) single crystals were determined to be 29 and 24 cm^{-1}/V, respectively,

under similar conditions in the literature, which are close to the value of 24.6 cm^{-1}/V on polycrystalline Pt film in this work.[38,39] This is an indication that the chemically deposited films are reasonable surrogates for flat single crystal surfaces in terms of Stark tuning measurements.

Quantitative analysis shows that the change in Stark tuning rate after correction is less than 8% when Stark tuning rates were determined using peaks with integrated area greater than 60% of the maximum value. This could serve as a rough gauge regarding the errors of using apparent Stark tuning rate values without correction. The deviation of the apparent Stark tuning rate from the intrinsic value increases rapidly if peaks with integrated areas less than 60% of the maximum value is used, where the dynamical coupling plays an increasingly important role in affecting the peak position.

Conclusion

In summary, we developed a general and reliable method to determine intrinsic Stark tuning rates of adsorbed CO on Cu surface by removing the coverage effect. A similar intrinsic Stark tuning rate of ~33 cm^{-1}/V was obtained on OD-Cu in different electrolyte pH of 7.2, 10.9 and 12.9, suggesting the pH independence of interfacial electric field in this pH range. Furthermore, the (electro)chemically deposited Cu films, i.e., Chem-Cu and OD-Cu, show similar intrinsic Stark tuning rate of ~33 cm^{-1}/V, while the particulate electrodes made by dropcasting catalyst inks, i.e., Den-Cu and Cu MPs, exhibit a similar rate of ~68 cm^{-1}/V under the same conditions. Based on the SEM images, we proposed that the electrode aggregate morphology, rather than the size and shape of individual particle, has a substantial impact on the interfacial electric field. The significantly increased intrinsic Stark tuning rates on Chem-Cu and Pt electrodes after being scraped off and then dropcast onto SEIRA active Au films further support the above hypothesis.

Author contributions

X.C., B.X. and Q.L. conceived and designed this project. X.C., H.X. and Y.X. conducted the in-situ SEIRAS experiments. Y.Z. collected the SEM images.

Acknowledgements

This work is supported by Beijing National Laboratory for Molecular Sciences and the National Natural Science Foundation of China (grant number 21872079). X.C. and B.X. acknowledge the support of the National Science Foundation CAREER Program (Award No. CBET-1651625).

Competing interests

The authors declare no competing interests.

Supporting Information

Experimental details, supporting data, and additional figures including spectro-electrochemical cell schematic and SEIRA spectra.

References

1 M. M. Waegele, C. M. Gunathunge, J. Li and X. Li, *J. Chem. Phys.*, 2019, **151**, 160902.

2 G. Hussain, L. Pérez-Martínez, J.-B. Le, M. Papasizza, G. Cabello, J. Cheng and A. Cuesta, *Electrochim. Acta*, 2019, **327**, 135055.

3 F. Che, J. T. Gray, S. Ha, N. Kruse, S. L. Scott and J.-S. McEwen, *ACS Catal.*, 2018, **8**, 5153-5174.

4 J. Li, X. Li, C. M. Gunathunge and M. M. Waegele, *Proc. Natl. Acad. Sci. USA*, 2019, **116**, 9220-9229.

5 S. Ringe, E. L. Clark, J. Resasco, A. Walton, B. Seger, A. T. Bell and K. Chan, *Energy Environ. Sci.*, 2019, **12**, 3001-3014.

6 A. S. Malkani, J. Li, N. J. Oliveira, M. He, X. Chang, B. Xu and Q. Lu, *Sci. Adv.*, 2020, **6**, eabd2569.

7 M. C. O. Monteiro, F. Dattila, B. Hagedoorn, R. Garcia-Muelas, N. Lopez and M. T. M. Koper, *Nat. Catal.*, 2021, DOI: 10.1038/s41929-021-00655-5.

8 A. Chattopadhyay and S. G. Boxer, *J. Am. Chem. Soc.*, 1995, **117**, 1449-1450.

9 D. K. Lambert, *Electrochim. Acta*, 1996, **41**, 623-630.

10 S. C. Chang, L.-W. H. Leung and M. J. Weaver, *J. Phys. Chem.*, 1989, **93**, 5341-5345.

11 J. D. Roth and M. J. Weaver, *Langmuir*, 1992, **8**, 1451-1458.

12 M. Dunwell, Q. Lu, J. M. Heyes, J. Rosen, J. G. Chen, Y. Yan, F. Jiao and B. Xu, *J. Am. Chem. Soc.*, 2017, **139**, 3774-3783.

13 M. C. Figueiredo, D. Hiltrop, R. Sundararaman, K. A. Schwarz and M. T. M. Koper, *Electrochim. Acta*, 2018, **281**, 127-132.

14 S. Holloway and J. K. Nørskov, *J. Electroanal. Chem. Interfacial Electrochem.*, 1984, **161**, 193-198.

15 M. T. M. Koper, R. A. van Santen, S. A. Wasileski and M. J. Weaver, *J. Chem. Phys.*, 2000, **113**, 4392-4407.

16 S. Zou and M. J. Weaver, *J. Phys. Chem.*, 1996, **100**, 4237-4242.

17 M. Su, J. C. Dong, J. B. Le, Y. Zhao, W. M. Yang, Z. L. Yang, G. Attard, G. K. Liu, J. Cheng, Y. M. Wei, Z. Q. Tian and J. F. Li, *Angew. Chem. Int. Ed.*, 2020, **59**, 23554-23558.

18 M. Osawa, K.-i. Ataka, K. Yoshii and T. Yotsuyanagi, *J. Electron Spectrosc. Relat. Phenom.*, 1993, **64-65**, 371-379.

19 W. Zhou, J. Guo, S. Shen, J. Pan, J. Tang, L. Chen, C. Au, S. Yin, *Acta Phys.-Chim. Sin.*, 2020, **36(3)**, 1906048.

20 R. M. Hammaker, S. A. Francis and R. P. Eischens, *Spectrochim. Acta*, 1965, **21**, 1295-1309.

21 P. Hollins and J. Pritchard, *Prog. Surf. Sci.*, 1985, **19**, 275-349.

22 X. Chang, A. Malkani, X. Yang and B. Xu, *J. Am. Chem. Soc.*, 2020, **142**, 2975-2983.

23 X. Chang, Y. Zhao and B. Xu, *ACS Catal.*, 2020, **10**, 13737-13747.

24 C. M. Gunathunge, V. J. Ovalle, Y. Li, M. J. Janik and M. M. Waegele, *ACS Catal.*, 2018, **8**, 7507-7516.

25 J. Salimon, R. M. Hernández-Romero and M. Kalaji, *J. Electroanal. Chem.*, 2002, **538-539**, 99-108.

26 J. Li, X. Chang, H. Zhang, A. S. Malkani, M. J. Cheng, B. Xu and Q. Lu, *Nat. Commun.*, 2021, **12**, 3264.

27 X. Jiang and M. J. Weaver, *Surf. Sci.*, 1992, **275**, 237-252.

28 Y. G. Yan, Q. X. Li, S. J. Huo, M. Ma, W. B. Cai and M. Osawa, *J. Phys. Chem. B*, 2005, **109**, 7900-7906.

29 P. Hollins and J. Pritchard, *Surf. Sci.*, 1979, **89**, 486-495.

30 E. Borguet and H. L. Dai, *J. Chem. Phys.*, 1994, **101**, 9080-9095.

31 S. E. Weitzner, S. A. Akhade, J. B. Varley, B. C. Wood, M. Otani, S. E. Baker and E. B. Duoss, *J. Phys. Chem. Lett.*, 2020, **11**, 4113-4118.

32 Y. Zhao, X. Chang, A. S. Malkani, X. Yang, L. Thompson, F. Jiao and B. Xu, *J. Am. Chem. Soc.*, 2020, **142**, 9735-9743.

33 M. Liu, Y. Pang, B. Zhang, P. De Luna, O. Voznyy, J. Xu, X. Zheng, C. T. Dinh, F. Fan, C. Cao, F. P. de Arquer, T. S. Safaei, A. Mepham, A. Klinkova, E. Kumacheva, T. Filleter, D. Sinton, S. O. Kelley and E. H. Sargent, *Nature*, 2016, **537**, 382-386.

34 M. Dunwell, J. Wang, Y. Yan and B. Xu, *Phys. Chem. Chem. Phys.*, 2017, **19**, 971-975.

35 B. Peng, Y.-G. Yan and W.-B. Cai, *Electrochim. Acta*, 2010, **55**, 8307-8311.

36 A. Loiudice, P. Lobaccaro, E. A. Kamali, T. Thao, B. H. Huang, J. W. Ager and R. Buonsanti, *Angew. Chem. Int. Ed.*, 2016, **55**, 5789-5792.

37 K. Manthiram, B. J. Beberwyck and A. P. Alivisatos, *J. Am. Chem. Soc.*, 2014, **136**, 13319-13325.

38 S. C. Chang, X. Jiang, J. D. Roth and M. J. Weaver, *J. Phys. Chem.*, 1991, **95**, 5378-5382.

39 L. Tian, J.-T. Li, J.-Y. Ye, C.-H. Zhen and S.-G. Sun, *J. Electroanal. Chem.*, 2011, **662**, 137-142.